Analysis of Transport Parameters in an Interacting Two-Band Model with Application to p^+-GaAs

B. W. Kim and A. Majerfeld

CONTENTS

I. INTRODUCTION

II. SEMICLASSICAL TRANSPORT IN THE INTERACTING TWO-BAND SYSTEM

III. EFFECTIVE RELAXATION TIME APPROACH

IV. SCATTERING MECHANISMS IN THE TWO-BAND SYSTEM

V. HOLE/HALL MOBILITIES AND HALL FACTOR FOR HEAVILY DOPED p-TYPE GaAs AT 300 K

VI. SUMMARY AND CONCLUSIONS

ACKNOWLEDGMENTS

APPENDICES

REFERENCES

ABSTRACT

We present a comprehensive derivation of the transport of holes involving an interacting two-valence-band system in terms of a generalized relaxation time approach. We solve a pair of semiclassical Boltzmann equations in a general way first, and then employ the conventional relaxation time concept to simplify the results. For polar optical phonon scattering, we develop a simple method to compensate for the inherent deficiencies in the relaxation time concept and apply it to calculate effective relaxation times separately for each band. Also, formulas for scattering rates and momentum relaxation times for the two-band model are presented for all the major scattering mechanisms for p-type GaAs for simple, practical mobility calculations. Finally, in the newly proposed theoretical framework, first-principles calculations for the Hall mobility and Hall factor of p-type GaAs at room temperature are carried out with no adjustable parameters in order to obtain a direct comparison between the theory and recent available experimental results, which would stimulate further analysis toward better understanding of the complex transport properties of the valence band. The calculated Hall mobilities show a general agreement with our experimental data for carbon doped p-GaAs samples in a range of degenerate hole densities. The calculated Hall factors show $r_H = 1.25 \sim 1.75$ over all hole densities ($2 \times 10^{17} \sim 1 \times 10^{20}\text{cm}^{-3}$) considered in the calculations.

I. INTRODUCTION

Recent improvements in transport calculations, especially for n-type materials, have made it possible to undertake quantitative comparisons with experiments. These have contributed greatly to elucidating particle scattering mechanisms, as well as to refining our knowledge of basic material constants [1]-[3]. For p-type semiconductors, the presence of the coupled heavy hole and light hole bands (the third split-off band is ignored provided that it is sufficiently separated from the two valence bands) introduces considerable complexity into transport calculations. It has been recognized that both intraband and interband scattering processes are important [4]-[6] and contribute significantly to the transport of charge carriers [7].

The standard way of handling the transport problem in interacting two-band systems is first to set up and then solve the two coupled Boltzmann equations. Although this can be carried out in principle by numerical computations using procedures such as the variational [8]-[10], iterative [11], [12], and Monte Carlo techniques [13], these methods could carry the disadvantages of intensive computational work and reduced physical insight into the problem.

In order to simplify the problem and provide a useful general understanding of the physics, several methods have been proposed based on the relaxation time (RT) concept. The simplest model in the relaxation time approximation (RTA) assumes that the two bands are completely decoupled [7], [14]. Although this decoupled approximation has been used in many cases [15], [16], it has proved to be extremely poor in the case of phonon scattering [6], [17], [18]. In order to include the presence of interband scattering, a more rigorous formula was presented [19], and later, as a simplified version of this formula, a "partial coupling approximation" was proposed [7]. However there has not been a completely general formulation for interacting bands.

Most recently, transport calculations have been performed for p-type materials by treating the heavy and light hole bands as a single heavy hole band, incorporating corrections to compensate for some possible deficiencies in this treatment [20], [21]. Although transport calculations based on such an approximation have shown reasonable agreement with experimental results, this approximation may not provide an adequate quantitative physical picture of the processes involved in two-band transport, such as the Hall factor, the contributions of each type of particle to the total mobility, and the importance of various interband scattering mechanisms. In order to obtain these information, it is necessary that the interactions between the two bands be explicitly taken into account in theoretical calculations.

The valence band system exhibits considerable warping which becomes severer at higher energies. The most important effect of the warping of energy surfaces shows in the Hall factor, r_H [7], which has been re-

flected by the fact that $r_H > 1$ by earlier works [12], [22]. The degenerate and warped valence bands make accurate calculations of r_H much more difficult than in the case of the conduction band. A first-order approximation can be obtained by treating the two bands as being decoupled, and each band with a constant effective mass. Such a calculation gives r_H factors at 300 K which can be greater than 2 for relatively pure materials [22]. An improved calculation, taking into account the energy band structure in the $\mathbf{k} \cdot \mathbf{p}$ approximation, also predicted that $r_H \cong 2$ for pure material at 300 K [12]. In this calculation, however, only lattice phonon scattering mechanisms were considered. As is well known, the mobility and carrier density from the Hall measurement are Hall mobility and Hall density, respectively. Thus, in order to properly interpret those measured quantities into the true carrier density and drift mobility, it becomes important to improve the theoretical calculations and to have more accurate r_H by including all the important scattering mechanisms and by treating those mechanisms properly.

In particular, analysis of transport in the case of highly degenerate hole densities requires proper incorporation of scattering mechanisms in the heavy and light hole bands. This has become recognized because during the last few years, high quality heavily doped epitaxial GaAs was achieved by different growth techniques employing C for the p-type dopant [23], [24]. This was used to improve the high frequency characteristics of the heterojunction bipolar transistor [25] and normal-light-incidence intersubband photoabsorption coefficient in quantum well structures [26]. In order to characterize and assess the quality of heavily doped p-type materials for design of heterojunction devices, it is important to obtain accurate carrier mobilities and the Hall factor [27]. Therefore, it is timely to examine transport theories further in order to have a better understanding of the physics and to provide a more accurate description of the transport properties of holes in heavily doped materials.

To this end, we present a comprehensive derivation based upon a generalized RT approach in which the conventional RT is conceptually extended to be a generalized transport parameter. We solve a pair of semiclassical Boltzmann equations in a general way first without using the conventional RT concept. Then the general solution is simplified using this concept. The formula derived in this process reduces in some cases to the forms given in previous work [7], [19]. We propose a simple method, which we will call "effective relaxation time (ERT)" method, using a variational technique to compensate for deficiencies in the RT concept for the polar optical phonon scattering mechanism. This was needed for the analysis, as for polar optical phonon scattering in an interactingve two-band system, the conventional variational method cannot provide, separately for each band, transport parameters accounting for intraband and interband scattering mechanisms.

We present formulas both for scattering rates and momentum RTs, in which interactions between the two bands are taken explicitly into account in the Born approximation, for simple, practical, mobility calculations. We treat the five most important scattering mechanisms for p-type GaAs: ionized impurity, polar optical phonon, nonpolar optical phonon, acoustic phonon, and piezoelectric scattering. We do not consider the plasmon scattering nor correction factors to account for carrier-carrier scattering. This is because the coupling of plasmon to the polar optical phonon modes should not have much effect on the overall hole mobility, and carrier-carrier scattering is greatly suppressed in the case of degenerate carrier concentrations [28] which is the case of primary interest in this work.

Using the theoretical framework presented in this paper, first-principles calculations for the Hall mobility and Hall factor for p-type GaAs is carried out with no adjustable parameters in order to obtain a rigorous, direct comparison between the theory and recent available experimental results, as this would be able to stimulate further analysis toward better understanding of the complex transport properties of the valence bands. The calculation is carried out for the range of hole densities $1 \times 10^{17} \sim 1 \times 10^{20} \mathrm{cm}^{-3}$; although transport properties in highly degenerate hole concentrations are of our primary interest, we include nondegenerate densities in the computation in order to simply provide some extended comparisons between the theory and experiments. Ionized impurity scattering, which dominates over other scattering mechanisms for highly degenerate hole densities, is treated both in the Born approximation (Brooks-Herring theory [29]) and in terms of the new phase-shift method, for the first time, which has recently been developed for the interacting two-band system [30]. We apply the ERT method to the polar optical phonon scattering mechanism. For the remaining scattering mechanisms, we apply the formulas based on the RTA and the Born approximation, derived in this paper for the interacting two-band system, as the validity in use of these approximations has been well established in the previous literature. Temperature is assumed to be 300 K for all calculations.

Finally, it should be noted that, in spite of the fact that there exist more rigorous, quantitative theoretical treatments, which have been developed mainly for materials with cubic symmetry and have contributed greatly to elucidating transport properties of silicon and germanium [31]-[39], the main intent of this work is to present a more complete and accurate transport model for p-type GaAs with emphasis on its practical engineering utility. For this purpose, we make a choice in models which can be as simple as they can produce results with reasonable accuracy, rather than the models as referred above with extremely intricate, difficult theoretical details for the complicated physical reality involved in the transport in the valence band. This was motivated by the fact that it has been recognized that many ob-

servable properties of holes in GaAs can be interpreted fairly well in terms of scalar (spherical equivalent) effective masses for the heavy- and light-hole bands, despite of the various complications of the ε-$\mathbf{k}$ relations for these two bands [40]. In addition, as the applied electric field marks out a preferential direction of charge-carrier motion, the directional dependence resulting from valence-band anisotropy would be alleviated by this preferential motion of holes.

The organization of this paper is as follows: in Section II, we solve the semiclassical Boltzmann equation for an interacting two band system. In Section III, we introduce a simple method, what we call effective relaxation time method, for a treatment of the polar optical phonon scattering. In Section IV, we present formulas for interband and intraband scattering rates and inverse relaxation times. In Section V, numerical computations for hole/Hall mobilities and Hall factor are performed.

II. SEMICLASSICAL TRANSPORT IN THE INTERACTING TWO-BAND SYSTEM

The scattering processes centered at band i $(i=1,\ 2)$ can be expressed as

$$S_i = S(\mathbf{k}_i,\ \mathbf{k}'_i) + S(\mathbf{k}_i,\ \mathbf{k}'_{i'}) \equiv S_{ii} + S_{ii'},$$
$$S'_i = S(\mathbf{k}'_i,\ \mathbf{k}_i) + S(\mathbf{k}'_{i'},\ \mathbf{k}_i) \equiv S'_{ii} + S'_{i'i}, \quad (1)$$

where $i \neq i'$ (hereafter we shall use this convention; for example, for band $i=1$, the band index i' designates band 2, and vice versa), $S(\mathbf{k}_i,\ \mathbf{k}'_j)$ is the differential scattering rate for the transition from initial state $\mathbf{k}$ in band i to final state $\mathbf{k}'$ in band j (outgoing scattering), and $S(\mathbf{k}'_j,\ \mathbf{k}_i)$ is that from state $\mathbf{k}'$ in band j to state $\mathbf{k}$ in band i (incoming scattering). This situation is depicted in Fig. 1.

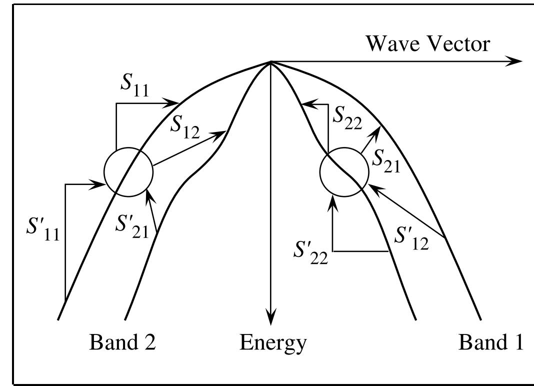

Fig. 1. Scattering processes in the interacting two-band system. S_{ij} and S'_{ij} represent outgoing and incoming scattering processes, respectively, from band i to band j.

Using the scattering rates defined in (1), a pair of Boltzmann equations can be written as

$$\begin{aligned}\frac{e}{\hbar}E\frac{\partial f_i}{\partial k_i}x_i = \int d\mathbf{k}'[&S'_{ii}(f'_i + x_i\chi_{ii}g'_i)(1-f_i-x_ig_i)\\ &+S'_{i'i}(f'_{i'}+x_i\chi_{ii'}g'_{i'})(1-f_i-x_ig_i)\\ &-S_{ii}(f_i+x_ig_i)(1-f'_i-x_i\chi_{ii}g'_i)\\ &-S_{ii'}(f_i+x_ig_i)(1-f'_{i'}-x_i\chi_{ii'}g'_{i'})],\end{aligned} \quad (2)$$

in an isotropic-band approximation, where χ_{ij} $(i,j = 1,2)$ is the cosine of the angle between either $\mathbf{k}_i$ and $\mathbf{k}'_j$ or $\mathbf{k}'_i$ and $\mathbf{k}_j$, the quan-

tities g and g' are the perturbation part of the nonequilibrium distribution function $\overline{f}(k_i)$ to first order in the external electric field $E(=|\mathbf{E}|)$, $x_i\,(x_i')$ is the cosine of the angle between $\mathbf{E}$ and $\mathbf{k}_i(\mathbf{k}_i')$, $f_i \equiv f(k_i)$, $f_i' = f(k_i')$; f is the equilibrium Fermi distribution function, $k_{i,j} = |\mathbf{k}_{i,j}|$, and we use the fact $\int x' S(\chi) d\mathbf{k}' = x \int \chi S(\chi) d\mathbf{k}'$, as S is independent of the azimuthal angle. The directional parameters used in (2) are shown in Fig. 2. In (2), we retain only first two terms in the perturbation expansion of $\overline{f}(k_i)$ under a weak external electric field $\mathbf{E}$; i.e.

$$\overline{f}(k_i) \cong f_i + x_i g_i \ \text{ and } \ \overline{f}(k_i') \cong f_i' + x_i' g_i'. \qquad (3)$$

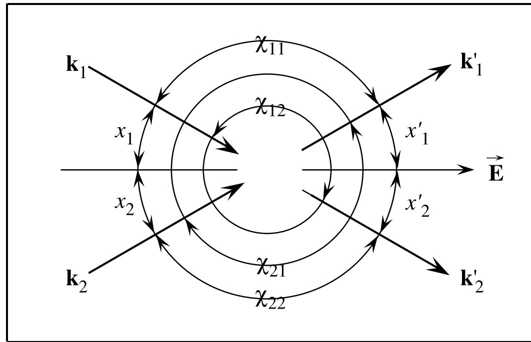

Fig. 2. Directional parameters for a scattering event. Initial wavevectors are designated by $\mathbf{k}_1$ and $\mathbf{k}_2$. Final wavevectors are designated by $\mathbf{k}_1'$ and $\mathbf{k}_2'$. $\mathbf{E}$ is the external electric field.

As in the isotropic band approximation the differential scattering rate can be expressed in terms of the magnitude of the wavevectors (k_i and k_j') and cosine of their angle χ_{ij}, all the functions involved in (2) can be expressed in terms of energy. Thus, hereafter we replace the wavevectors by corresponding energies for those functions. In this approximation, g and g' for both elastic and inelastic scattering can be assumed to take the form [41]:

$$\begin{aligned} g &\equiv g(\varepsilon) = -\frac{eE\tau(\varepsilon)}{\hbar}\frac{\partial f(\varepsilon)}{\partial k}, \\ g' &\equiv g(\varepsilon') = -\frac{eE\tau(\varepsilon')}{\hbar}\frac{\partial f'}{\partial k'} \\ &= g(\varepsilon)\frac{\partial f'/\partial k'}{\partial f/\partial k}[1 + F(\tau,\ \varepsilon' - \varepsilon)], \end{aligned} \qquad (4)$$

where

$$F(\tau_i,\ \varepsilon_i' - \varepsilon_i) = \frac{1}{\tau_i}\sum_{n=1}^{\infty}\frac{1}{n!}\frac{\partial^n \tau_i}{\partial \varepsilon_i^n}(\varepsilon_i' - \varepsilon_i)^n. \qquad (5)$$

We note that, even though the valence band is not isotropic except near the band maxima, we take this form of (4) to be valid up to the hole density considered in this paper.

Integrating (2) over x_1 and x_2, respectively, gives

$$\begin{aligned} \int d\mathbf{k}'[S_{ii}' f_i'(1 - f_i) + S_{i'i}' f_{i'}'(1 - f_i) \\ - S_{ii} f_i(1 - f_i') - S_{ii'} f_i(1 - f_{i'}')] = 0. \end{aligned} \qquad (6)$$

This equation describes the detailed balance in the interacting two-band system and should be satisfied for any final state $\mathbf{k}'$. Thus, the integrand of (6) vanishes. If we make the physically reasonable assumption that the intraband and interband scattering rates separately obey the detailed balance condition, we then obtain

$$S_{ij}' f_i' = S_{ji} f_j \frac{1 - f_i'}{1 - f_j}. \qquad (7)$$

On the other hand, integrating (2) over x_1 and x_2 of the resultant equations multiplied by x_1 and x_2, respectively, gives

$$-\frac{e}{\hbar}E\frac{\partial f_i}{\partial k_i} = \int d\mathbf{k}'\{S_{ii}'[f_i' g_i - \chi_{ii}(1 - f_i)g_i']$$

$$+S'_{i'i}[f'_{i'}g_i - \chi_{ii'}(1-f_i)g'_{i'}]$$
$$+S_{ii}[(1-f'_i)g_i - \chi_{ii} f_i g'_i]$$
$$+S_{ii'}[(1-f'_{i'})g_i - \chi_{ii'} f_i g'_{i'}]\}. \quad (8)$$

Replacing g' and S' by g and S, respectively, in (8), using the second equations of (4) and (7), and solving for g_1 and g_2, we obtain the solution exact to first order in the electric field E:

$$\tau_i = \frac{q_{nom}}{q_{den}}, \quad (9)$$

where

$$q_{nom} = (q_{i'i'} + q_{i'i} + \triangle q'_{i'i'}) - (q'_{ii'} + \triangle q'_{ii'}),$$
$$q_{den} = (q_{ii} + q_{ii'} + \triangle q'_{ii})(q_{i'i'} + q_{i'i} + \triangle q'_{i'i'}) - (q'_{ii'} + \triangle q'_{ii'})(q'_{i'i} + \triangle q'_{i'i}),$$
$$q_{ii} = \int d\mathbf{k}' S_{ii} \frac{(1-f'_i)}{(1-f_i)} \left(1 - \sqrt{\frac{\varepsilon'_i m_i}{\varepsilon_i m'_i}} \chi_{ii}\right)$$
$$= \pi \left(\frac{2m'_i}{\hbar^2}\right)^{3/2} \int \cos\theta d\theta \int \sqrt{\varepsilon'_i} d\varepsilon'_i \times S_{ii} \frac{(1-f'_i)}{(1-f_i)} \left(1 - \sqrt{\frac{\varepsilon'_i m_i}{\varepsilon_i m'_i}} \cos\theta\right),$$
$$q_{ii'} = \int d\mathbf{k}' S_{ii'} \frac{(1-f'_{i'})}{(1-f_i)}$$
$$= \pi \left(\frac{2m'_{i'}}{\hbar^2}\right)^{3/2} \int \cos\theta d\theta \int \sqrt{\varepsilon'_{i'}} d\varepsilon'_{i'} \times S_{ii'} \frac{(1-f'_{i'})}{(1-f_i)},$$
$$q'_{ii'} = -\int d\mathbf{k}' S_{ii'} \frac{(1-f'_{i'})}{(1-f_i)} \sqrt{\frac{\varepsilon'_{i'} m_i}{\varepsilon_i m'_{i'}}} \chi_{ii'}$$
$$= -\pi \left(\frac{2m'_{i'}}{\hbar^2}\right)^{3/2} \int \cos^2\theta d\theta \int \sqrt{\varepsilon'_{i'}} d\varepsilon'_{i'} \times S_{ii'} \frac{(1-f'_{i'})}{(1-f_i)} \sqrt{\frac{\varepsilon'_{i'} m_i}{\varepsilon_i m'_{i'}}},$$
$$\triangle q'_{ij} = -\int d\mathbf{k}' S_{ij} \frac{(1-f'_j)}{(1-f_i)} \sqrt{\frac{\varepsilon'_j m_i}{\varepsilon_i m'_j}} \times F(\tau_j,\ \varepsilon'_j - \varepsilon_j)\chi_{ij}$$
$$= -\pi \left(\frac{2m'_j}{\hbar^2}\right)^{3/2} \int \cos^2\theta d\theta \int \sqrt{\varepsilon'_j} d\varepsilon'_j \times S_{ij} \frac{(1-f'_j)}{(1-f_i)} \sqrt{\frac{\varepsilon'_j m_i}{\varepsilon_i m'_j}} F(\tau_j,\ \varepsilon'_j - \varepsilon_j). \quad (10)$$

Here, we set $\chi = \cos\theta$; ε_i (ε'_i) and m_i (m'_i), respectively, are the energy and effective mass for the initial (final) state in band i, and the first and the second indices for the quantities, q, q', and $\triangle q'$, designate initial and the final bands involved in the transition, respectively.

It should be noted that τ_i in the above equations is not a well-defined quantity but a "generalized" transport parameter from the conventional RT, as $\triangle q'_{ij}$ contains τ_j itself. If $\triangle q'_{ij}$ of (10) vanishes or can be neglected, e.g. in cases that either a scattering process is randomizing (i.e., $\int d\Omega' S_{ij}\tau_{ij} = 0$, where $d\Omega'$ is an element of solid angle for the direction of $\mathbf{k}'$) or the energy emitted/absorbed by a particle in a collision process is small compared with the initial energy of the particle (i.e., $F \approx 0$), then τ_i becomes a well-defined quantity as the conventional RTs. If these conditions are not satisfied, to improve the quality of numerical computations, one can use an iteration technique in which one starts by neglecting $\triangle q'_{ij}$ to get zeroth order RTs in terms of energy ε and then uses these values for the evaluation of $\triangle q'_{ij}$ to obtain higher order τ_i. This approach is closely related to the iteration method of [11]. We may consider this higher order τ_i as "generalized RTs" from their physical similarity to the conventional RTs.

For elastic scattering, $\triangle q'_{ij} = 0$ as $F = 0$, as

Table 1. Glossary of symbols I.

e = particle charge	D_0 = optical phonon deformation potential
k_B = Boltzmann constant	E_1 = acoustic phonon deformation potential
T = temperature in [K]	K_{av} = average electrochemical coupling coefficient
n_I = density of ionized impurity scatterers	s = velocity of acoustic mode
ε_0 = free space dielectric constant	$q = \|\mathbf{q}\|$ = acoustic phonon wave vector
ε_s = low frequency relative dielectric constant	ω_q = frequency of acoustic mode (= sq)
ε_∞ = high frequency relative dielectric constant	ρ = density of the semiconductor material
$\mathbf{k}(\mathbf{k}')$ = wave vector of the initial (final) state	V_c = volume of the crystal
$\varepsilon(\varepsilon')$ = energy of the initial (final) state	$\chi_{ij} = \cos\theta_k$, θ_k is the angle between $\mathbf{k}_i$ and $\mathbf{k}'_j$ or $\mathbf{k}_j$ and $\mathbf{k}'_i$
$m(m')$ = effective mass of initial (final) state	$\mathbf{E}$ = external electric field
$M = m'/m$ = ratio of the final- to initial - effective masses	$x(x_i)$ = cosine of the angle between $\mathbf{k}(\mathbf{k}_i)$ and $\mathbf{E}$
f = Fermi distribution function; $f = f(k)$, $f' = f(k')$	$x'(x'_i)$ = cosine of the angle between $\mathbf{k}'(\mathbf{k}'_i)$ and $\mathbf{E}$
$N = 1/[e^{\hbar\omega/k_BT} - 1]$ = Boson distribution function	i, i' = band indices for band 1 and band 2; $i \neq i'$
$\hbar\omega_0$ = LO-phonon energy at the zone center	q_s = inverse screening length
γ = index of phonon process;	W_{ij} = scattering rate from band i to band j
$\gamma = +1$ for emission and $\gamma = -1$ for absorption	q_{ii}, $q_{ii'}$, $q'_{ii'}$ = inverse relaxation times

can be seen from (5). Thus, τ_i becomes well-defined and is given by

$$\tau_i = \frac{q_{i'i'} + q_{i'i} - q'_{ii'}}{(q_{ii} + q_{ii'})(q_{i'i'} + q_{i'i}) - q'_{ii'}q'_{i'i}}. \tag{11}$$

We note that (11) has the same form as given in [19]. If we can approximate $q'_{ii'} \approx 0$, based on the fact that interband scattering may be considered as large angle scattering so that $|q'_{ii'}| \ll |q_{ii} + q_{ii'}|$, (11) can be further simplified to become a "partial coupling approximation" [7] :

$$\frac{1}{\tau_i} = \int d\mathbf{k}' S_{ii}(1 - \chi_{ii}) + \int d\mathbf{k}' S_{ii'} \equiv \frac{1}{\tau_{ii}} + \frac{1}{\tau_{ii'}}. \tag{12}$$

It should be noted that, when using this approximation, the interband scattering terms, $1/\tau_{ii'}$, should not be weighted with the factor $1 - \chi$.

III. EFFECTIVE RELAXATION TIME APPROACH

Another way to approach the non-randomizing inelastic scattering problem would be to consider an ERT approach. We begin with setting $\triangle q'_{ij} = 0$ to obtain well-defined τ_1 and τ_2 for each band. Then we correct the resultant relaxation times by multiplying by correction factors $\triangle\tau_i$ (i.e., $\tau_{ERT,i} = \triangle\tau_i \cdot \tau_i$) to implicitly include higher order corrections in the quantity $\triangle q'_{ii}$. This procedure results in neglecting the corrections in $\triangle q'_{ii'}$, from the interband scattering event. This, however, would not make any noticeable effect on the result as $|\triangle q'_{ii'}| \ll |\triangle q'_{ii}|$, which can be explained by the same reason as that used to obtain (12) from (11). Therefore, interband interactions are treated within RTA and intraband interactions are treated beyond RTA. In this section, we present this approach for the polar optical phonon scattering process by following the variational technique [8]-[10]. We note that since we explicitly neglect the corrections from $\triangle q'_{ii'}$ $(i \neq i')$ and since each band can be treated as an independent band in obtaining $\triangle\tau_i$, band indices will be omitted in this section for notational simplicity. The symbols and notations used in the equations are given in Tables 1 and 2.

In the presence of an external electric field $\mathbf{E}$ in the $\hat{x}$-direction, the collision term due to polar optical phonon scattering is given by (Appendix A)

$$\left[\frac{\partial \overline{f}}{\partial t}\right]_C = -\left(\frac{\hbar k}{m}\frac{\partial f}{\partial \varepsilon}x\right)\frac{e^2\hbar\omega_0 m}{16\pi\varepsilon_0\hbar^2}\left(\frac{1}{\varepsilon_\infty}-\frac{1}{\varepsilon_s}\right)\frac{1}{\varepsilon}$$

$$\times\frac{1-f'}{1-f}[P_1(\varepsilon,\ \varepsilon')C(\varepsilon) - P_2(\varepsilon,\ \varepsilon')C(\varepsilon')] \times[(N+1)\delta_e + N\delta_a] = -\left(\frac{\hbar k}{m}\frac{\partial f}{\partial \varepsilon}x\right)\frac{e^2\hbar\omega_0 m}{16\pi\varepsilon_0\hbar^2}\times\left(\frac{1}{\varepsilon_\infty}-\frac{1}{\varepsilon_s}\right)\frac{1}{\varepsilon}L(C), \quad (13)$$

where δ_e and δ_a describe energy conservation for emission (subscript e) and absorption (subscript a), respectively, functions P_1 and P_2 are given in Appendix A, and a collision operator L, which is a function of $C(\varepsilon)$, is defined as

$$L(C) \equiv \frac{1-f'}{1-f}[P_1(\varepsilon,\ \varepsilon')C(\varepsilon) - P_2(\varepsilon,\ \varepsilon')C(\varepsilon')] \times[(N+1)\delta_e + N\delta_a]. \quad (14)$$

Here $C(\varepsilon)$ is the first correction term in the

Table 2. Glossary of symbols II.

$$q_s^2 = \frac{e^2 p}{2\varepsilon k_B T}\frac{F_{-1/2}(\eta_F)}{F_{+1/2}(\eta_F)},$$

$$F_r(\eta_F) = \int_0^\infty \frac{x^r\,dx}{1+e^{x-\eta_F}},\ \eta_F = \frac{\varepsilon_F}{k_B T}$$

$$A = \frac{k'^2+k^2+q_s^2}{2kk'} = \frac{K'M+K+Q}{2\sqrt{KK'M}}$$

$$B = \frac{k'^2+k^2}{2kk'} = \frac{K'M+K}{2\sqrt{KK'M}}$$

$$C = \frac{k'm}{km'} = \frac{\sqrt{K'}}{\sqrt{KM}}$$

$$K = \frac{\hbar^2k^2}{2mk_BT},\ K' = \frac{\hbar^2k'^2}{2m'k_BT}$$

$$Q = \frac{\hbar^2q_s^2}{2mk_BT},\ W = \frac{\hbar\omega_0}{k_BT},\ S = \frac{ms^2}{2k_BT},$$

$$z = \frac{\hbar sq}{k_BT}$$

expansion of $\overline{f}$ (see (A3)). The RTA requires $\tau(k) \cong \tau(k')$ and dictates $\triangle q' = 0$. Comparing (3) and (4) with (A3), the corresponding requirement in (13) is given by

$$C(\varepsilon') \cong \frac{k'm}{km'} C(\varepsilon) \equiv \frac{k'm}{km'} C_0(\varepsilon) = \frac{k'}{k} C_0(\varepsilon), \quad (15)$$

where C_0 designates an RT solution of $C(\varepsilon)$, and $m = m'$ in a parabolic-band approximation (effective masses of the initial and final states are the same in a parabolic band).

Thus, the RTA solution to (13) can be obtained by the equation

$$\frac{1}{C_0(\varepsilon)} \left[\frac{\partial \overline{f}}{\partial t} \right]_C = \frac{1}{C_0(\varepsilon)} \left(-\frac{\hbar k}{m} \frac{\partial f}{\partial \varepsilon} x e E \right) = -\left(\frac{\hbar k}{m} \frac{\partial f}{\partial \varepsilon} x \right) \frac{e^2 \hbar \omega_0 m}{16 \pi \varepsilon_0 \hbar^2} \times \left(\frac{1}{\varepsilon_\infty} - \frac{1}{\varepsilon_s} \right) \frac{1}{\varepsilon} L_0(\varepsilon), \quad (16)$$

where $L_0(\varepsilon)$ is defined as

$$L_0(C) \equiv \frac{1-f'}{1-f} \left[P_1(\varepsilon, \varepsilon') - P_2(\varepsilon, \varepsilon') \frac{k'}{k} \right] \times [(N+1)\delta_e + N\delta_a]. \quad (17)$$

From (16), $C_0(\varepsilon)$ is given by

$$C_0(\varepsilon) = \left[\frac{e^2 \hbar \omega_0 m}{16 \pi \varepsilon_0 \hbar^2} \left(\frac{1}{\varepsilon_\infty} - \frac{1}{\varepsilon_s} \right) \right]^{-1} \varepsilon \frac{eE}{L_0(\varepsilon)}. \quad (18)$$

On the other hand, the collision operator L can be written as

$$L(C) = \left[\frac{e^2 \hbar \omega_0 m}{16 \pi \varepsilon_0 \hbar^2} \left(\frac{1}{\varepsilon_\infty} - \frac{1}{\varepsilon_s} \right) \right]^{-1} \varepsilon e E. \quad (19)$$

The linear finite difference equation of (14) can be solved by defining

$$C(\varepsilon) = \left[\frac{e^2 \hbar \omega_0 m}{16 \pi \varepsilon_0 \hbar^2} \left(\frac{1}{\varepsilon_\infty} - \frac{1}{\varepsilon_s} \right) \right]^{-1} e E C^{(1)}, \quad (20)$$

where $C^{(1)}$ is the solution of (Appendix B)

$$\varepsilon = L(C^{(1)}). \quad (21)$$

The correction factor $\triangle\tau$ and τ_{ERT} can be defined, respectively, as

$$\triangle\tau(\varepsilon) \equiv \frac{C(\varepsilon)}{C_0(\varepsilon)} = \frac{L_0(\varepsilon)}{\varepsilon} C^{(1)}, \quad (22)$$

and

$$\tau_{ERT}(\varepsilon) = \tau(\varepsilon) \cdot \triangle\tau(\varepsilon), \quad (23)$$

as these lead to the correct current equation:

$$\begin{aligned} j &= \frac{ne^2 E}{m} \frac{\int \tau_{ERT}(\varepsilon) f(1-f) \varepsilon^{3/2} d\varepsilon}{\int f(1-f) \varepsilon^{3/2} d\varepsilon} \\ &= \frac{2em}{3\pi^2 \hbar^4} \int \varepsilon \frac{eE\hbar}{m} k \tau_{ERT} \frac{\partial f}{\partial \varepsilon} d\varepsilon \\ &= \frac{2em}{3\pi^2 \hbar^3} \int_0^\infty \varepsilon C(\varepsilon) \frac{\partial f}{\partial \varepsilon} d\varepsilon \\ &= -\frac{e}{4\pi^3} \int \nu_x f d^3 k, \end{aligned} \quad (24)$$

where ν_x is the velocity of the carrier in the $\hat{x}$-direction, and we used the relation

$$\frac{eE\hbar}{m} k \tau(k) \frac{\partial f}{\partial \varepsilon} = C_0(\varepsilon) \frac{\partial f}{\partial \varepsilon}. \quad (25)$$

To see the significance of this correction to the RTA for polar optical phonon scattering, we apply this formula to p-type GaAs at room temperature. Figure 3 shows correction factors $\triangle\tau$ (averaged over energy) as a function of hole density. Figure 4 shows the effect of this correction on the polar optical phonon mobility by plotting $\mu_{po}(\tau_{ERT})$ and $\mu_{po}(\tau)$. At lower hole densities ($< 10^{18} \text{cm}^{-3}$), the RTA underestimates polar optical phonon mode scattering rates and for degenerate hole

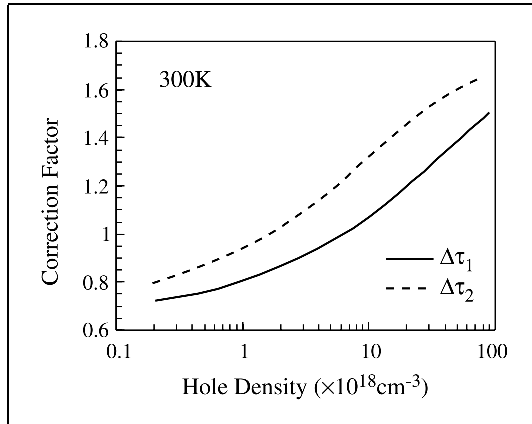

Fig. 3. Correction factors $\triangle\tau(\varepsilon)$ to the conventional relaxation times due to the use of the relaxation time approximation for polar optical phonon scattering, where $\triangle\tau_1$ and $\triangle\tau_2$ refer to heavy and light holes, respectively.

densities ($> 10^{18}\mathrm{cm}^{-3}$) it overestimates them. An analogous result has been reported for n-type GaAs [10].

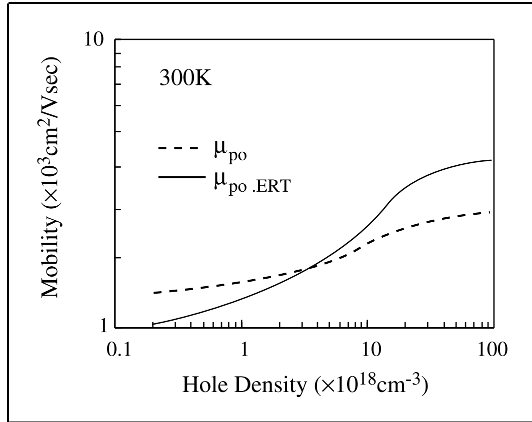

Fig. 4. Comparison of the polar optical phonon mobilities calculated by the relaxation time approximation and the effective relaxation time method.

IV. SCATTERING MECHANISMS IN THE TWO-BAND SYSTEM

In this section we present formulas for intraband and interband scattering rates (W_{ii}, $W_{ii'}$, $i \neq i'$) and the inverse relaxation times ($q_{ii}, q_{ii'}, q'_{ii'}$) for the interacting two-band system. The inverse relaxation times are defined in (10), and the scattering rate is given by

$$W_{ij} = \int S_{ij} d\mathbf{k}' = \frac{V_c}{8\pi^3} \int \frac{2\pi}{\hbar} |M_{ij}(\mathbf{k}, \mathbf{k}')|^2 \times \delta[\varepsilon(\mathbf{k}') - \varepsilon(\mathbf{k})] d\mathbf{k}', \qquad (26)$$

where V_c is the crystal volume. Here, $M_{ij}(\mathbf{k}, \mathbf{k}')$ is the matrix element between the Bloch wavefunctions $\psi_i(\mathbf{k}, \mathbf{r}) = u_i(\mathbf{k}, \mathbf{r}) e^{i\mathbf{k}\cdot\mathbf{r}}$ for a transition included by a perturbing potential V_{ij} from the state $\mathbf{k}$ of band i to the state $\mathbf{k}'$ of band j :

$$\begin{aligned} M_{ij}(\mathbf{k}, \mathbf{k}') &= \int \psi_j^*(\mathbf{k}', \mathbf{r}) V_{ij} \psi_i(\mathbf{k}, \mathbf{r}) d\mathbf{r} \\ &\cong v_{ij}(\mathbf{k}' - \mathbf{k}) \\ &\quad \times \int_{unit\ cell} u_j^*(\mathbf{k}', \mathbf{r}) u_i(\mathbf{k}, \mathbf{r}) d\mathbf{r}, \qquad (27) \end{aligned}$$

where v_{ij} is the Fourier-transformed form of V_{ij}, and cell periodic functions $u_i(\mathbf{k}, \mathbf{r})$ are normalized over a unit cell. The integration over the cell periodic functions in (27) represents the anisotropy of scattering due to the symmetry properties of the wavefunctions of Bloch holes. The square modulus of this integration, with averaging over the spin states s_i and s_j (s_i, $s_j = \pm 1/2$), is defined as the overlap function [14]:

$$G_{ij}(\mathbf{k}, \mathbf{k}') = \frac{1}{2} \sum_{s_i, s_j} \left| \int_{unit\ cell} u_j^*(\mathbf{k}', s_j, \mathbf{r}) \right.$$

$$\times u_i(\mathbf{k},\, s_i,\, \mathbf{r}) d\mathbf{r} \Big|^2 . \quad (28)$$

We neglect the k-dependence of the overlap functions by using their forms in the limit that $\mathbf{k}$ and $\mathbf{k}'$ become zero, which are given by [14]

$$G_{11}(\theta_k) = G_{22}(\theta_k) = \frac{1}{4}[1 + 3\cos^2(\theta_k)],$$
$$G_{12}(\theta_k) = G_{21}(\theta_k) = \frac{3}{4}\sin^2(\theta_k), \quad (29)$$

where θ_k is the angle between $\mathbf{k}$ and $\mathbf{k}'$. Using (27) and (28), the scattering rate of (26) is given by

$$W_{ij} = \frac{V_c}{8\pi^3} \int \frac{2\pi}{\hbar} \left| v_{ij}(\mathbf{k}' - \mathbf{k}) \right|^2 G_{ij}(\mathbf{k},\, \mathbf{k}') \times \delta[\varepsilon(\mathbf{k}') - \varepsilon(\mathbf{k})] d\mathbf{k}'. \quad (30)$$

The specific forms of $|v(\mathbf{k}' - \mathbf{k})|^2$ for the scattering mechanisms of interest in p-GaAs, as discussed in the Introduction, are given in this section: In the derivation of the formulas, (1) we use the Born approximations; (2) we take into account screening of charged carriers; and (3) for the optical phonon modes scattering, we use the Einstein model in which the energy of the optical mode is independent of the lattice wavevector. In this model, we consider only energy conservation, because if energy conservation is satisfied we can always find a wave vector for which momentum conservation is satisfied; (4) for the acoustic phonon modes, we use the Debye approximation; and (5) the scattering probability is assumed to be independent of the azimuthal angle φ.

The scattering rates and inverse relaxation times can be easily calculated by substituting (29) and $|v(\mathbf{k}' - \mathbf{k})|^2$ into (30) and (10). Therefore only final forms needed for numerical computation for these transport quantities are presented in below. The notation used in the formulas is shown in Tables 1 and 2. The first and second indices for W's and q's designate the bands which contain the initial state and the final state, respectively. Once the inverse RTs are known, the momentum relaxation times for band 1 and band 2, τ_1 and τ_2, can be calculated by (9).

1. Ionized Impurity Scattering

$$|v(\mathbf{k}' - \mathbf{k})|^2 = n_I V_c \left(\frac{Ze^2}{V_c \varepsilon_s} \frac{1}{|\mathbf{k}' - \mathbf{k}|^2 + q_s^2} \right)^2,$$

$$W_{ii'} = q_{ii'} = \frac{3 n_I e^4 \sqrt{M}}{64\sqrt{2}\pi \varepsilon_s^2 \sqrt{m} (k_B T)^{3/2}} \times \frac{1}{K^{3/2}} \left[2A \ln \frac{|A+1|}{|A-1|} - 4 \right],$$

$$q_{ii} = \frac{n_I e^4}{64\sqrt{2}\pi \varepsilon_s^2 \sqrt{m} (k_B T)^{3/2}} \frac{1}{K^{3/2}} \times \left[(3A-1)^2 \ln \frac{A+1}{A-1} - 2\left(9A - 6 + \frac{4}{A+1} \right) \right],$$

$$q'_{ii'} = -\frac{3 n_I e^4 \sqrt{M}}{64\sqrt{2}\pi \varepsilon_s^2 \sqrt{m} (k_B T)^{3/2}} \frac{C}{K^{3/2}} \times \left[6A + (3A^2 - 1) \ln \frac{|A-1|}{|A+1|} \right], \quad (31)$$

where

$$A = \frac{M + 1 + Q/K}{2\sqrt{M}} \quad \text{and} \quad C = \frac{1}{\sqrt{M}}. \quad (32)$$

We note that $\triangle q' = 0$ because $F = 0$ as seen from (5), and that $W_{ii'} = q_{ii'}$ as the quantity $(1 - f')/(1 - f)$ included in $q_{ii'}$ becomes unity

for elastic scattering (compare (26) and (10)). The fact that $\triangle q' = 0$ explains that the relaxation times are well defined for elastic scattering even in the interacting twoband systems.

2. Polar Optical Phonon Scattering

$$|v(\mathbf{k}'-\mathbf{k})|^2 = \frac{e^2\hbar\omega_0}{2V_c\varepsilon_0}\left(\frac{1}{\varepsilon_\infty}-\frac{1}{\varepsilon_s}\right) \times \frac{|\mathbf{k}'-\mathbf{k}|^2}{(|\mathbf{k}'-\mathbf{k}|^2+q_s^2)^2}\left\{\begin{matrix} N \\ N+1\end{matrix}\right\},$$

$$W_{ii} = \frac{e^2\sqrt{k_BT}\sqrt{m}}{32\sqrt{2}\pi\hbar^2\varepsilon_0}\frac{W}{\sqrt{K}}\left(\frac{1}{\varepsilon_\infty}-\frac{1}{\varepsilon_s}\right) \times \left\{\begin{matrix} N \\ N+1\end{matrix}\right\}\left[(9A^2-6AB+1)\ln\frac{|A+1|}{|A-1|} -2\frac{9A^3-6A^2B-5A+2B}{A^2-1}\right],$$

$$W_{ii'} = \frac{3e^2\sqrt{k_BT}M\sqrt{m}}{32\sqrt{2}\pi\hbar^2\varepsilon_0}\frac{W}{\sqrt{K}}\left(\frac{1}{\varepsilon_\infty}-\frac{1}{\varepsilon_s}\right)\left\{\begin{matrix} N \\ N+1\end{matrix}\right\} \times\left[(3A^2-2AB-1)\ln\frac{|A-1|}{|A+1|} +2(3A-2B)\right],$$

$$q_{ii} = \frac{e^2\sqrt{k_BT}\sqrt{m}}{32\sqrt{2}\pi\hbar^2\varepsilon_0}\frac{W}{\sqrt{K}}\left(\frac{1}{\varepsilon_\infty}-\frac{1}{\varepsilon_s}\right)\left\{\begin{matrix} N \\ N+1\end{matrix}\right\} \times\left[(12A^3-9A^2B-9A^2+6AB+2A-B-1) \times\ln\frac{|A-1|}{|A+1|}+2\left((9A^2-6AB-6A+3B+2) +\frac{(A-B)(3A^2+1)}{A+1}\right)\right],$$

$$q_{ii'} = \frac{3e^2\sqrt{k_BT}M\sqrt{m}}{32\sqrt{2}\pi\hbar^2\varepsilon_0}\frac{W}{\sqrt{K}}\left(\frac{1}{\varepsilon_\infty}-\frac{1}{\varepsilon_s}\right) \times\frac{1-f(K-\gamma W)}{1-f(K)}\left\{\begin{matrix} N \\ N+1\end{matrix}\right\} \times\left[(3A^2-2AB-1)\ln\frac{|A-1|}{|A+1|} +2(3A-2B)\right],$$

$$q'_{ii'} = -\frac{3e^2\sqrt{k_BT}M\sqrt{m}}{32\sqrt{2}\pi\hbar^2\varepsilon_0}\frac{W}{\sqrt{K}}\left(\frac{1}{\varepsilon_\infty}-\frac{1}{\varepsilon_s}\right) \times\frac{1-f(K-\gamma W)}{1-f(K)}\left\{\begin{matrix} N \\ N+1\end{matrix}\right\} \times C\left[(4A^3-(3A^2-1)B-2A)\ln\frac{|A-1|}{|A+1|} +2\left(4A^2-3AB-\frac{2}{3}\right)\right], \quad (33)$$

where the upper part in the brace corresponds to phonon absorption and the lower part to phonon emission, $N \equiv N(\omega_0)$, and

$$A = \frac{(M+1)K-M\gamma W+Q}{2\sqrt{MK(K-\gamma W)}},$$

$$B = \frac{(M+1)K-M\gamma W}{2\sqrt{MK(K-\gamma W)}},$$

and,

$$C = \frac{\sqrt{K-\gamma W}}{\sqrt{MK}}, \quad (34)$$

with $M=1$ for intraband scattering.

It should be noted that this scattering mechanism has non-vanishing $\triangle q'$, and, thus, it may cause some considerable error if $\triangle q'$ is ignored. One simple method to incorporate this quantity into the computation is using the effective relaxation time method as introduced in Sec. III.

3. Nonpolar Optical phonon Scattering

$$|v(\mathbf{k}'-\mathbf{k})^2| = \frac{\hbar D_0^2}{2V_c\rho\omega_0}\left\{\begin{matrix} N \\ N+1\end{matrix}\right\},$$

$$W_{ii} = \frac{D_0^2 m^{3/2}}{2\sqrt{2}\pi\hbar^2\rho\sqrt{k_BT}}\frac{\sqrt{K-\gamma W}}{W}\left\{\begin{matrix} N \\ N+1\end{matrix}\right\},$$

$$W_{ii'} = \frac{D_0^2 (Mm)^{3/2}}{2\sqrt{2}\pi\hbar^2\rho\sqrt{k_BT}}\frac{\sqrt{K-\gamma W}}{W}\left\{\begin{matrix} N \\ N+1\end{matrix}\right\},$$

$$q_{ii} = \frac{D_0^2 m^{3/2}}{2\sqrt{2}\pi\hbar^2\rho\sqrt{k_B T}} \frac{\sqrt{K}}{W} \begin{Bmatrix} N \\ N+1 \end{Bmatrix},$$
$$q_{ii'} = \frac{D_0^2 (Mm)^{3/2}}{2\sqrt{2}\pi\hbar^2\rho\sqrt{k_B T}} \frac{\sqrt{K-\gamma W}}{W} \times \frac{1-f(K-\gamma W)}{1-f(K)} \begin{Bmatrix} N \\ N+1 \end{Bmatrix}. \quad (35)$$

Although this scattering mechanism is inelastic, this scattering is randomizing over the solid angle for the direction of $\mathbf{k}'$, which makes $\triangle q' = 0$, so that the generalized relaxation times become well defined as in the case of the elastic scattering mechanism. In addition, $q'_{ii'} = 0$ for the same reason of the randomizing nature of this scattering mechanism.

4. Acoustic Deformation Potential Scattering

$$|v(\mathbf{k}'-\mathbf{k})|^2 = \frac{\hbar E_1^2}{2V_c\rho s^2}\omega_q \begin{Bmatrix} N \\ N+1 \end{Bmatrix},$$
$$W_{ii} = \frac{E_1^2 m^{5/2}\sqrt{k_B T}}{16\sqrt{2}\pi\hbar^4\rho S^2} \frac{1}{\sqrt{K}} \int_{z_1}^{z_2} dz z^2 \begin{Bmatrix} N \\ N+1 \end{Bmatrix} \times \frac{1}{4}\left[1 + \frac{\frac{3}{4}\left(2-\gamma\frac{z}{K}-\frac{z^2}{4KS}\right)^2}{\left(1-\gamma\frac{z}{K}\right)}\right],$$
$$W_{ii'} = \frac{E_1^2 M m^{5/2}\sqrt{k_B T}}{16\sqrt{2}\pi\hbar^4\rho S^2} \frac{1}{\sqrt{K}} \int_{z_1}^{z_2} dz z^2 \begin{Bmatrix} N \\ N+1 \end{Bmatrix} \times \frac{3}{4}\left[1 - \frac{\frac{1}{4}\left((1+M)-\gamma M\frac{z}{K}-\frac{z^2}{4KS}\right)^2}{M\left(1-\gamma\frac{z}{K}\right)}\right],$$
$$q_{ii} = \frac{E_1^2 m^{5/2}\sqrt{k_B T}}{16\sqrt{2}\pi\hbar^4\rho S^2} \frac{1}{\sqrt{K}} \int_{z_1}^{z_2} dz z^2 \begin{Bmatrix} N \\ N+1 \end{Bmatrix} \frac{1}{4} \times \left[1 + \frac{\frac{3}{4}\left(2-\gamma\frac{z}{K}-\frac{z^2}{4KS}\right)^2}{\left(1-\gamma\frac{z}{K}\right)}\right] \times \left[1 - \frac{\frac{1}{2}\left(2-\gamma\frac{z}{K}-\frac{z^2}{4KS}\right)}{\left(1-\gamma\frac{z}{K}\right)^{1/2}}\right],$$
$$q_{ii'} = \frac{E_1^2 M m^{5/2}\sqrt{k_B T}}{16\sqrt{2}\pi\hbar^4\rho S^2} \frac{1}{\sqrt{K}} \int_{z_1}^{z_2} dz z^2 \times \frac{1-f(K-\gamma W)}{1-f(K)} \begin{Bmatrix} N \\ N+1 \end{Bmatrix} \times \frac{3}{4}\left[1 - \frac{\frac{1}{4}\left((1+M)-\gamma M\frac{z}{K}-\frac{z^2}{4KS}\right)^2}{M\left(1-\gamma\frac{z}{K}\right)}\right],$$
$$q'_{ii'} = -\frac{E_1^2 M m^{5/2}\sqrt{k_B T}}{16\sqrt{2}\pi\hbar^4\rho S^2} \frac{1}{\sqrt{K}} \int_{z_1}^{z_2} dz z^2 \times \frac{1-f(K-\gamma W)}{1-f(K)} \begin{Bmatrix} N \\ N+1 \end{Bmatrix} C \times \frac{3}{4}\left[1 - \frac{\frac{1}{4}\left((1+M)-\gamma M\frac{z}{K}-\frac{z^2}{4KS}\right)^2}{M\left(1-\gamma\frac{z}{K}\right)}\right] \times \left[\frac{\frac{1}{2}\left((1+M)-\gamma M\frac{z}{K}-\frac{z^2}{4KS}\right)}{\sqrt{M}\left(1-\gamma\frac{z}{K}\right)^{1/2}}\right], \quad (36)$$

where C is given by

$$C = \frac{1}{\sqrt{M}}\left(1-\gamma\frac{z}{K}\right)^{1/2}. \quad (37)$$

The computation of the δ-function representing the energy and momentum conservations and the integration limits, z_1 and z_2, are given in Appendix C.

It should be noted that, rigorously speaking, this scattering mechanism produces nonvanishing $\triangle q'$. However, since the energy emitted/absorbed by a particle involved in this type of scattering process is small compared with the initial energy of the particle, one may neglect $\triangle q'$.

5. Piezoelectric Scattering

$$|v(\mathbf{k}'-\mathbf{k})|^2 = \frac{\hbar}{2V_c\rho}\left(\frac{ee_{14}}{\varepsilon}\right)^2\left[\frac{12}{35}\frac{1}{s_l} + \frac{16}{35}\frac{1}{s_t}\right]\frac{1}{q}\frac{|\mathbf{k}'-\mathbf{k}|^4}{(|\mathbf{k}'-\mathbf{k}|^2+q_s^2)^2}\left\{\begin{matrix} N \\ N+1 \end{matrix}\right\}$$
$$\cong \frac{\hbar e^2 K_{av}^2}{2V_c\rho\varepsilon}\frac{s}{q}\frac{q^4}{(q^2+q_s^2)^2}\left\{\begin{matrix} N \\ N+1 \end{matrix}\right\},$$

$$W_{ii} = \frac{e^2 K_{av}^2\sqrt{m}\sqrt{k_BT}}{4\sqrt{2}\pi\hbar^2\varepsilon}\frac{1}{\sqrt{K}}\int_{z_1}^{z_2} dz\frac{z^4}{(z^2+4QS)^2} \times\left\{\begin{matrix} N \\ N+1 \end{matrix}\right\}\frac{1}{4}\left[1+\frac{\frac{3}{4}\left(2-\gamma\frac{z}{K}-\frac{z^2}{4KS}\right)^2}{\left(1-\gamma\frac{z}{K}\right)}\right],$$

$$W_{ii'} = \frac{e^2 K_{av}^2 M\sqrt{m}\sqrt{k_BT}}{4\sqrt{2}\pi\hbar^2\varepsilon}\frac{1}{\sqrt{K}} \times\int_{z_1}^{z_2} dz\frac{z^4}{(z^2+4QS)^2}\left\{\begin{matrix} N \\ N+1 \end{matrix}\right\} \times\frac{3}{4}\left[1-\frac{\frac{1}{4}\left((1+M)-\gamma M\frac{z}{K}-\frac{z^2}{4KS}\right)^2}{M\left(1-\gamma\frac{z}{K}\right)}\right],$$

$$q_{ii} = \frac{e^2 K_{av}^2\sqrt{m}\sqrt{k_BT}}{4\sqrt{2}\pi\hbar^2\varepsilon}\frac{1}{\sqrt{K}}\int_{z_1}^{z_2} dz\frac{z^4}{(z^2+4QS)^2} \times\left\{\begin{matrix} N \\ N+1 \end{matrix}\right\}\frac{1}{4}\left[1+\frac{\frac{3}{4}\left(2-\gamma\frac{z}{K}-\frac{z^2}{4KS}\right)^2}{\left(1-\gamma\frac{z}{K}\right)}\right] \times\left[1-\frac{\frac{1}{2}\left(2-\gamma\frac{z}{K}-\frac{z^2}{4KS}\right)}{\left(1-\gamma\frac{z}{K}\right)^{1/2}}\right],$$

$$q_{ii'} = \frac{e^2 K_{av}^2 M\sqrt{m}\sqrt{k_BT}}{4\sqrt{2}\pi\hbar^2\varepsilon}\frac{1}{\sqrt{K}} \times\int_{z_1}^{z_2} dz\frac{z^4}{(z^2+4QS)^2}\frac{1-f(K-\gamma W)}{1-f(K)} \times\left\{\begin{matrix} N \\ N+1 \end{matrix}\right\} \times\frac{3}{4}\left[1-\frac{\frac{1}{4}\left((1+M)-\gamma M\frac{z}{K}-\frac{z^2}{4KS}\right)^2}{M\left(1-\gamma\frac{z}{K}\right)}\right],$$

$$q'_{ii'} = -\frac{e^2 K_{av}^2 M\sqrt{m}\sqrt{k_BT}}{4\sqrt{2}\pi\hbar^2\varepsilon}\frac{1}{\sqrt{K}} \times\int_{z_1}^{z_2} dz\frac{z^4}{(z^2+4QS)^2}\frac{1-f(K-\gamma W)}{1-f(K)} \times\left\{\begin{matrix} N \\ N+1 \end{matrix}\right\}C \times\frac{3}{4}\left[1-\frac{\frac{1}{4}\left((1+M)-\gamma M\frac{z}{K}-\frac{z^2}{4KS}\right)^2}{M\left(1-\gamma\frac{z}{K}\right)}\right] \times\left[\frac{\frac{1}{2}\left((1+M)-\gamma M\frac{z}{K}-\frac{z^2}{4KS}\right)}{\sqrt{M}\left(1-\gamma\frac{z}{K}\right)^{1/2}}\right], \quad (38)$$

where s_l and s_t, respectively, are the spherical average velocities of the longitudinal "l" and transverse "t" phonons, the integration limits, z_1 and z_2, are the same as in the acoustic phonon scattering case, e_{14} is the piezoelectric constant, the quantity C, in the equation for $q'_{ii'}$, is given by (37). In the first equation of (38) both the longitudinal and transverse sound velocities are replaced by an average sound velocity $s^2 = \frac{1}{3}s_l^2 + \frac{2}{3}s_t^2$, and K_{av} is an average electrochemical coupling coefficient, defined to be

$$K_{av}^2 = \frac{(e_{14})^2}{\varepsilon}\left(\frac{12}{35C_L}+\frac{16}{35C_T}\right), \quad (39)$$

where the constants C_L and C_T are given by

$$C_L = \frac{1}{5}(3C_{11}+2C_{12}+4C_{44})$$
and
$$C_T = \frac{1}{5}(C_{11}-C_{12}+3C_{44}), \quad (40)$$

with the strain constants C_{ij}. We note that $\triangle q'$ can be neglected for the same reason as in the acoustic-deformation-potential scattering case.

V. HOLE/HALL MOBILITIES AND HALL FACTOR FOR HEAVILY DOPED p-TYPE GaAs AT 300 K

For the analysis of hole transport in p-type GaAs, the heavy hole band can be considered to be nearly parabolic and the light hole band to be nearly isotropic in the energy region near the top of the valence band [40]. Thus, in numerical computations, we use an energy-independent effective mass for the heavy hole band, while for the light hole band we use an energy-dependent effective mass calculated using the $\mathbf{k}\cdot\mathbf{p}$ method [42]. This is necessary especially for highly degenerate carrier densities as holes occupy a higher energy region where the light hole band becomes highly non-parabolic. We note that the energy dependence of the density-of-states effective mass does not stem from band anisotropy but from band non-parabolicity.

For hole/Hall mobilities and Hall factor calculations, we use no adjustable parameters and no compensation (i.e. $N_D^+/N_A^- = 0$). We include five of the most important scattering mechanisms for GaAs, as discussed previously. Several important issues, such as Hall factor (r_H), screening of charge carriers, and overlap functions are taken into account. We apply the phase-shift method recently developed for the interacting two-band system [30] for a more proper treatment of ionized impurity scattering than the Born approximation. We use the ERT method for polar optical phonon scattering to reduce the error caused by the use of the RT concept for non-randomizing inelastic scattering. For the remaining three scattering mechanisms we use the formulas presented in the previous section, in which the interband scattering mechanism is taken explicitly into account in the RTA. The validity in use of RTA for those scattering mechanisms has been well established in the previous literature. The parameters used in these calculations are shown in Table 3.

Table 3. List of materials parameters [4], [34].

$m_h = 0.51 m_0$ (heavy hole mass)
$m_l = 0.088 m_0$ at $\mathbf{k} = 0$ (light hole mass)
m_0 = free electron mass
$\varepsilon_s = 12.9$
$\varepsilon_\infty = 10.92$
$\hbar\omega_0 = 0.035 eV$
$\rho = 5360$ kg/m^3
Spherical average of velocity of sound:
$s_l = 4730$ m/s ; longitudinal
$s_t = 3340$ m/s ; transverse
$s = 3860$ m/s ; total
Elastic constant:
$C_{11} = 11.88 \times 10^{10}$ N/m^2
$C_{12} = 5.38 \times 10^{10}$ N/m^2
$C_{44} = 5.94 \times 10^{10}$ N/m^2
Deformation Potential Constants:
$E_1 = 5.6$ eV
Optical-phonon coupling constants:
$(DK)^2 = 1.58 \times 10^{22}$ eV^2/m^2

Once the relaxation times were obtained for each band, the hole drift mobility in band i were calculated by $\mu_i = e < \tau_i(\varepsilon) > /m_i$, where <> denotes an average over carrier energies (in our numerical computations, the upper limit for this integration was $10k_BT$ above the Fermi energy or $10k_BT$ into the band). The combined hole drift mobility is obtained from $\mu = (p_1\mu_1 + p_2\mu_2)/(p_1 + p_2)$, where p_1 and p_2 are the hole densities in band 1 and band 2, respectively. Once drift mobilities and Hall factors for each band are calculated, the combined Hall mobility and Hall factor of the two band system can be calculated as (D2) and (D3) in Appendix D.

Figure 5 plots calculated r_H factors for p-type GaAs as a function of Hall density ($p = 2 \times 10^{17} \sim 1 \times 10^{20}$ cm^{-3}). The Hall factors obtained by using the Born approximation for ionized impurity scattering show values ranging from $r_H \cong 0.87$ to 1.5 (Fig. 5a). The phase-shift method gives r_H values which are significantly greater than unity ($r_H \cong 1.25 \sim 1.75$) for Hall densities considered in this calculation (Fig. 5b). As the phase-shift method is more accurate than the Born approximation for treating ionized impurity scattering, it is reasonable to rely on the results from the phase-shift method, which are also closer to previous results [12], [22]. Therefore, it can be concluded that the usual assumption $r_H \cong 1$ would intoduce some errors in the interpretation of Hall data.

Figure 6 shows calculated hole drift mobilities as a function of hole densities ($p = 2 \times 10^{17} \sim 1 \times 10^{20}$ cm^{-3}) with various methods. In this figure, B and P designate, respectively, employment of the Born approximation and phase-shift method for ionized impurity scattering; E indicates the use of the ERT method for polar optical phonon mode scattering. It also shows contributions of heavy holes

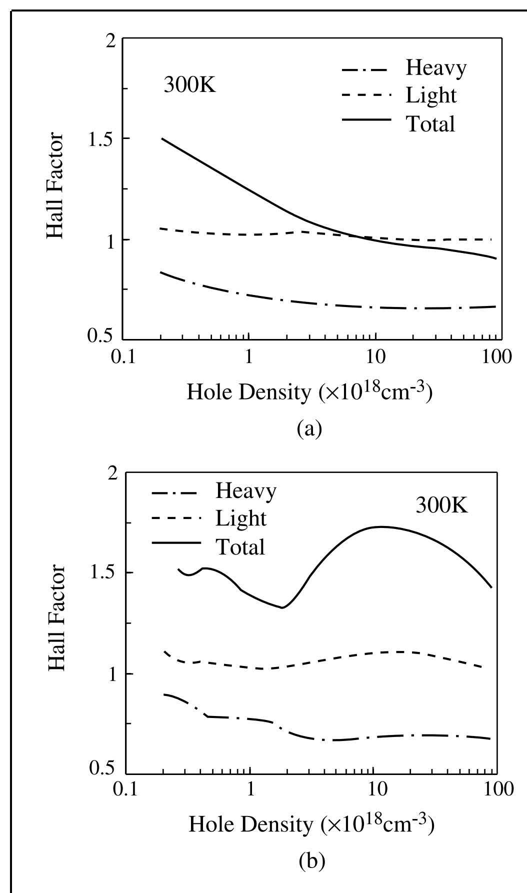

Fig. 5. Hall factors of p-type GaAs, calculated using (a) the Born approximation and (b) the phase-shift method for ionized impurity scattering. The effective relaxation time method was used for polar optical phonon scattering.

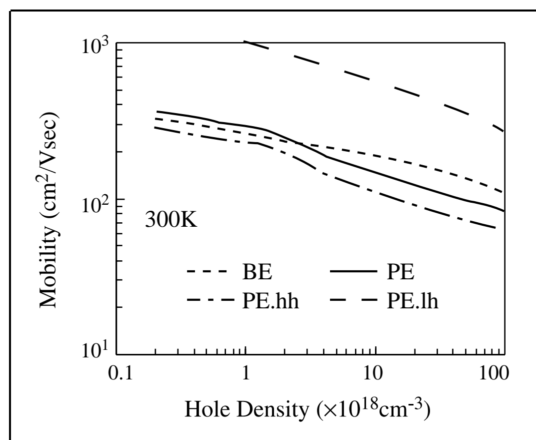

Fig. 6. Comparison of hole drift mobilities calculated by various methods; B, P, and E designate the use of the Born approximation, the phase-shift method, and the effective relaxation time method, respectively. The contributions of heavy holes (PE.hh) and light holes (PE.lh) to the total hole mobility (PE) are also shown in the case using the phase-shift method.

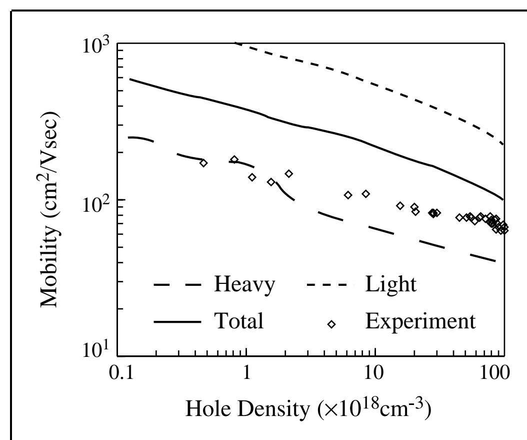

Fig. 7. Hall mobility at 300 K vs. Hall density calculated using the phase-shift and the effective relaxation time methods. The contributions of heavy and light hole mobilities to total mobilities are shown.

(PE.hh) and light holes (PE.lh) to the total hole mobility (PE) in the case of using the phase-shift method. As seen from this figure, the presence of the light hole band (PE.lh) causes a considerable increase in the hole drift mobility by 25 ∼ 35% (i.e., from the heavy hole mobility (PE.hh) to the total mobility (PE) in the figure) depending on hole concentrations; and the Born approximation overestimates the overall ionized impurity scattering rates for hole concentrations less than $3 \times 10^{18}\text{cm}^{-3}$ and underestimates the rates by approximately 25 ∼ 40% for concentrations greater than this value. This was previously noted by other researchers [8].

Figure 7 shows the theoretical Hall mobilities and the contributions by the heavy and light holes in the case of PE. The figure shows that the calculated Hall mobilities are turned out to be somewhat higher than the experimental mobilities depending on Hall concentrations; e.g., 30% higher at a Hall density of $1 \times 10^{20}\text{cm}^{-3}$. The experimental data were obtained from carbon-doped p-type GaAs samples grown by AP-MOVPE using CCl_4 [23]. In a purely computational point of view, this discrepancy between the theory and the experiment can be viewed as a result of the incorporation of the Hall factor into the calculation in a sense that if r_H were set to be unity as it has been done in most of previous works, then the agreement would become excellent in the region of highly degenerate hole concentrations, in which the omission of carrier-carrier scattering can be well justified. This can be seen clearly by comparing the experi-

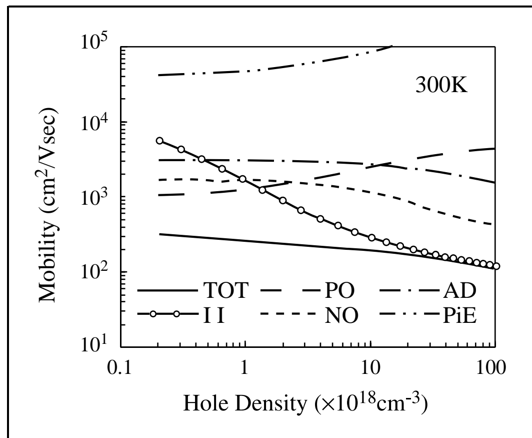

Fig. 8. Contributions of individual scattering mechanisms to the total hole drift mobility: The phase-shift method was used for ionized impurity scattering and the effective relaxation time method was used for polar optical phonon scattering. The scattering mechanisms included are ionized impurity (II), polar optical phonon (PO), nonpolar optical phonon (NO), acoustic deformation (AD), and piezoelectric (PiE) scattering.

mental data with the calculated hole mobilities of Fig. 6. The result stimulates a further investigation so that the discrepancy can be clarified in such ways whether there may be other scattering mechanisms (e.g. neutral impurity scattering) or materials properties (e.g. compensation) not taken into account in the calculation. Elimination of approximations with valence-band nonparabolicity and anisotropy make some contribution to reducting the disparity.

Figure 8 shows the contributions of various scattering mechanisms to the total hole mobility. As seen from this figure, at low hole densities, polar optical phonon scattering mechanism dominates, while at degenerate hole densities ionized impurity scattering mechanism is the mobility-limiting factor to the total hole mobility.

VI. SUMMARY AND CONCLUSIONS

We have presented a comprehensive derivation for hole transport in the interacting two-band system (p-type materials with the heavy hole and light hole bands). A pair of Boltzmann equations were set up and solved, first in a most general way, in terms of a generalized relaxation time. Then the general solution was simplified using the conventional relaxation time concept. We showed that in specific cases our general solution reduces to those that have been previously reported, including the so called partial coupling approximation. We also showed that when the partial coupling approximation is used, the inverse interband momentum relaxation time $1/\tau_{ii'}$ (i, i' =band index; $i' \neq i$) should not be weighted with the factor $1-\cos\theta_k$, where θ_k is the angle between the initial and the final wavevectors, which is in contradiction to what has been done in the previous literature.

For non-randomizing inelastic polar optical phonon scattering, we have presented a simple (ERT) method, developed along the lines of the conventional variational technique, to compensate for the use of the RTA and to calculate respective effective relaxation times

for each band. We investigated the validity of the RTA for this type of scattering. The results showed that RTA underestimates the scattering rate for nondegenerate hole densities and overesimates the scattering rate for degenerate densities. For example, for $p \cong 2 \times 10^{17}$ cm^{-3}, the mobility calculated by RTA is approximately 34% higher than the value obtained by ERT, and for $p \cong 2 \times 10^{20}$ cm^{-3} the mobility by RTA is about 37% lower than that by ERT. An analogous result has been reported for n-type GaAs [10]. As the RTA result deviates far from that of the ERT, it can be concluded that the use of RTA may not be well justified for the polar optical phonon scattering mechanism in the range of hole concentrations considered in this paper.

For simple, practical mobility calculations, we derived, taking explicitly into account interactions between the two bands, formulas both for scattering rates and momentum RTs in the Born approximation for five the most important scattering mechanisms for p-GaAs.

Using the theoretical framework presented in this paper, a first-principles numerical computation was performed for the hole/Hall mobilities and the Hall factor over a range of hole densities $p = 2 \times 10^{17} \sim 1 \times 10^{20}$ cm^{-3}. Although transport properties in highly degenerate hole concentrations, in which the omission of carrier-carrier scattering can be well justified, are of our primary interest, we include non-degenerate densities in the computation in order to simply provide extended comparisons between the theory and experiments. We included all the most important scattering mechanisms, as mentioned above, for p-type GaAs. We took into account the Hall factor to directly compare the theoretical Hall mobility with the experimental data. We also considered other important effects on hole transport, such as the nonparabolicity of the light-hole band, overlap functions, and screening. We applied the phase-shift method, recently developed for interacting two-band systems, to calculate the relaxation times due to ionized impurity scattering for each band. As compared with the result obtained using the phase-shift method, the use of the Born approximation overestimates the hole drift mobility for hole concentrations less than 3×10^{18} cm^{-3} and underestimates it by $25 \sim 40\%$ for concentrations greater than this value. In addition, for highly-degenerate hole concentrations greater than 4×10^{19} cm^{-3}, the ionized impurity scattering mechanism makes the greatest contribution (over 90%) to the total hole drift mobility. This leads to a conclusion that the use of the phase-shift method for ionized impurity scattering mechanism is necessary for highly degenerate hole concentrations.

Regarding the contribution of each band to the total hole mobility, it was shown that the presence of the light hole band causes a considerable increase in the hole drift mobilities by $25 \sim 35\%$ depending on hole concentrations. This may indicate that inclusion of the light hole band through taking explicitly into account the interband scattering mechanism would be important in transport calculations.

The Hall factor obtained using the Born approximation for ionized impurity scattering showed values ranging from $r_H \cong 0.87$ to 1.5. The phase-shift method gave $r_H \cong 1.25 \sim 1.75$ over all hole densities considered in this calculation. As the phase-shift method is more accurate than the Born approximation, it is appropriate to use the result from the phase-shift method, which is also closer to those obtained in earlier works. Therefore, we conclude that the usual assumption, $r_H \cong 1$, can introduce some errors in interpreting true hole densities and drift mobilities from experimental Hall data.

The calculated Hall mobilities are turned out to be somewhat higher than the experimental mobilities obtained from carbon-doped p-type GaAs samples depending on Hall concentrations; i.e., 30% higher at Hall concentration of 1×10^{20} cm^{-3}. In a purely computational point of view, this discrepancy between the theory and the experiment can be viewed as a result of the incorporation of the Hall factor into the calculation in a sense that if r_H were set to be unity as it has been done in most of previous works, then the agreement would become excellent in the region of highly degenerate hole concentrations, in which the omission of carrier-carrier scattering can be well justified. This can be seen clearly by comparing the experimental data with the calculated hole mobilities of Fig. 6. The result stimulates a further investigation so that the discrepancy can be clarified: it is expected that incorporation of neutral impurity scattering and compensation for degenerate hole densities and carrier-carrier scattering effect for non-degenerate hole densities would lead to an improvement in theoretical fitting to experimental observations. In addition, elimination of some crucial approximations employed in our theoretical treatment in association with the valence-band structure will provide a complete picture of hole transport for GaAs and would considerably reduce the disparity between theory and experiment. This might require computational effort beyond that needed for simple, practical engineering purposes. However, when this becomes necessary, the effects of band nonparabolicity and anisotropy can be taken into account exactly in the treatment of the scattering mechanisms and in the solution of the Boltzmann equation by incorporating into our theoretical frame the theoretical formulations with a full consideration of the valence-band properties [31], [37]. These investigations have been being carried out by the authors. However, we expect that, although limited by the use of approximations in the present theoretical frame, the present work is still of significant practical value as a reasonable engineering study on transport parameters in p-type GaAs.

Finally, we note that hole mobilities of p-GaAs at 77 K were found to be lower than those at 300 K for hole densities $p \cong 1 \times 10^{18} \sim 10^{19}$ cm^{-3} [23]. This phenomenon has been observed by other investigators [43]. A possible explanation for the strong reduction in hole mobility at low temperatures will be presented

elsewhere based on a simple theoretical model.

ACKNOWLEDGMENTS

We thank Dr. J. R. Lowney for initial discussions. We would like to acknowledge Dr. K. C. Park, Mr. S. R. Kang, and Dr. C. H. Yim for their long-standing support of this work.

APPENDIX A

In the presence of an external electric field $\mathbf{E}$ in the $\hat{x}$-direction, the Boltzmann equation for the non-equilibrium distribution function $\overline{f}(\mathbf{k})$ takes the form

$$\left(\frac{\hbar k}{m} xeE\right) \frac{\partial f(k)}{\partial \varepsilon} = \left[\frac{\partial \overline{f}}{\partial t}\right]_c, \qquad \text{(A1)}$$

where

$$\left[\frac{\partial \overline{f}}{\partial t}\right]_c = \int d^3k' [S' f'(1-f) - S f(1-f')], \qquad \text{(A2)}$$

and x is the cosine of the angle between $\mathbf{k}$ and the electric field $\mathbf{E}$. Assuming $\overline{f}$ to take the form

$$\overline{f} = f - \Phi(\mathbf{k}) \frac{\partial f}{\partial \varepsilon}, \qquad \text{(A3)}$$

and neglecting terms of order Φ^2, the collision term for polar optical phonon scattering becomes

$$\begin{aligned}\left[\frac{\partial \overline{f}}{\partial t}\right]_c &= \int d^3k' S \frac{1-f'}{1-f} \frac{\partial f}{\partial \varepsilon} (\Phi - \Phi') \\ &= \left(\frac{\hbar k}{m} \frac{\partial f}{\partial \varepsilon} x\right) \frac{e^2 \hbar \omega_0 m}{16\pi \varepsilon_0 \hbar^2} \left(\frac{1}{\varepsilon_\infty} - \frac{1}{\varepsilon_s}\right) \frac{1}{\varepsilon_0} C(\varepsilon) \\ &\quad \times \int dk' \int_{-1}^{+1} d\chi \frac{b-\chi}{(a-\chi)^2} (1 - c\chi) \frac{1-f'}{1-f} \\ &\quad \times [(N+1)\delta(k'-k_e) + N\delta(k'-k_a)],\end{aligned} \qquad \text{(A4)}$$

where we assume Φ to take the form

$$\begin{aligned}\Phi &= \Phi(\mathbf{k}) = xC(\varepsilon), \\ \Phi' &= \Phi(\mathbf{k}') = x'C(\varepsilon') = x\chi C(\varepsilon'),\end{aligned} \qquad \text{(A5)}$$

and

$$a = \frac{\varepsilon' + \varepsilon + \frac{\hbar^2 q_s^2}{2m}}{2\sqrt{\varepsilon\varepsilon'}}, \quad b = \frac{\varepsilon' + \varepsilon}{2\sqrt{\varepsilon\varepsilon'}}, \quad c = \frac{C(\varepsilon')k'}{C(\varepsilon)k}, \qquad \text{(A6)}$$

$$k = |\mathbf{k}|, \quad k' = |\mathbf{k}'|, \quad \varepsilon = \varepsilon(k), \quad \varepsilon' = \varepsilon(k'),$$

and k_e and k_a are the solutions for k' to the energy conservation equation

$$\varepsilon(\mathbf{k}') = \varepsilon(\mathbf{k} - \gamma\mathbf{q}) = \varepsilon(\mathbf{k}) + \gamma h\omega_0,$$

with $\gamma = 1$ for phonon emission and $\gamma = -1$ for absorption. In (A5), x' is the cosine of the angle between $\mathbf{k}'$ and $\mathbf{E}$, χ is the cosine of the angle between $\mathbf{k}$ and $\mathbf{k}'$, and we use the law of cosines and the fact that the integration over the azimuthal angle makes the terms multiplied by this angle vanish. In (A5), the integration over k' can be performed easily using the delta function property, and the integration over χ gives

$$\begin{aligned}&\left\{2\left[1 + \frac{a(a-b)}{a^2-1}\right] + (2a-b)\ln\frac{|a-1|}{|a+1|}\right\} \\ &\quad \times \frac{C(\varepsilon')}{C(\varepsilon)} - \left\{\frac{2(a-b)}{a^2-1} + \ln\frac{|a-1|}{|a+1|}\right\} \\ &= P_2(\varepsilon, \varepsilon')\frac{C(\varepsilon')}{C(\varepsilon)} - P_1(\varepsilon, \varepsilon').\end{aligned} \qquad \text{(A7)}$$

APPENDIX B

For the present problem the variational principle is described as follows. Let h_1 and h_2

be any two functions of ε, and let

$$(h_1,\, h_2) = \int_0^\infty h_1 L(h_2) \frac{\partial f}{\partial \varepsilon} d\varepsilon, \qquad \text{(B1)}$$

where L is given by (13). Then solution $C^{(1)}$ to (21) can be determined by maximizing $(C^{(1)}, C^{(1)})$, subject to the auxiliary condition

$$\int_0^\infty C^{(1)} L(C^{(1)}) \frac{\partial f}{\partial \varepsilon} d\varepsilon = \int_0^\infty \varepsilon C^{(1)} \frac{\partial f}{\partial \varepsilon} d\varepsilon. \quad \text{(B2)}$$

It can be shown that $(h_1, h_2) = (h_2, h_1)$ and $(h_1, h_2) > 0$ to comply with the variational principle. In order to solve this equation, $C^{(1)}$ is expanded as a polynomial in powers of the energy:

$$C^{(1)}(\varepsilon) = \sum_{r=0}^{\infty} C_r^{(1)} \varepsilon^r, \qquad \text{(B3)}$$

which satisfies the infinite set of linear equations:

$$\sum_{r=0}^{\infty} d_{rs} C_s^{(1)} - \alpha_r^{(1)} = 0 \quad (r = 0, 1, 2, 3, \cdots), \quad \text{(B4)}$$

where

$$\begin{aligned}
\alpha_r^{(n)} &= \int_0^\infty \varepsilon^{n+r} \frac{\partial f}{\partial \varepsilon} d\varepsilon \\
&= -(r+n)(k_B T)^{r+n} F_{r+n-1}(\xi), \\
F_k(\xi) &= \int_0^\infty \frac{x^k dx}{e^{x-\xi}+1}, \\
d_{rs} &= (\varepsilon^r,\, \varepsilon^s) = \int_0^\infty \varepsilon^r L(\varepsilon^s) \frac{\partial f}{\partial \varepsilon} d\varepsilon \\
&= -\frac{N+1}{k_B T} \int_0^\infty d\varepsilon (\varepsilon + \hbar\omega_0)^r f(\varepsilon + \hbar\omega_0) \\
&\quad \times [1 - f(\varepsilon)][P_1(\varepsilon + \hbar\omega_0, \varepsilon)(\varepsilon + \hbar\omega_0)^s \\
&\quad - P_2(\varepsilon + \hbar\omega_0, \varepsilon)\varepsilon^s] \\
&= -\frac{N}{k_B T} \int_0^\infty d\varepsilon\, \varepsilon^r f(\varepsilon)[1 - f(\varepsilon + \hbar\omega_0)] \\
&\quad \times [P_1(\varepsilon, \varepsilon + \hbar\omega_0)\varepsilon^s - P_2(\varepsilon, \varepsilon + \hbar\omega_0) \\
&\quad \times (\varepsilon + \hbar\omega_0)^s],
\end{aligned}$$

$$\begin{aligned}
L(\varepsilon^s) &= \frac{1 - f(\varepsilon - \hbar\omega_0)}{1 - f(\varepsilon)} (N+1) \\
&\quad \times [P_1(\varepsilon, \varepsilon - \hbar\omega_0)\varepsilon^s \\
&\quad - P_2(\varepsilon, \varepsilon - \hbar\omega_0)(\varepsilon - \hbar\omega_0)^s] \\
&\quad + \frac{1 - f(\varepsilon + \hbar\omega_0)}{1 - f(\varepsilon)} N [P_1(\varepsilon, \varepsilon + \hbar\omega_0)\varepsilon^s \\
&\quad - P_2(\varepsilon, \varepsilon + \hbar\omega_0)(\varepsilon + \hbar\omega_0)^s]. \qquad \text{(B5)}
\end{aligned}$$

One can see that $d_{rs} = d_{sr}$, which the variational principle requires. This symmetry stems from the facts that

$$P_{1,2}(x, y) = P_{1,2}(y, x)$$

and

$$\begin{aligned}
&(N+1) f(\varepsilon + \hbar\omega_0)[1 - f(\varepsilon)] \\
&= N f(\varepsilon)[1 - f(\varepsilon + \hbar\omega_0)].
\end{aligned}$$

APPENDIX C

The integration limits, z_1 and z_2, are determined as follows [4]. Energy and momentum conservation can be written, respectively, as

$$\frac{\hbar^2 k'^2}{2m'} = \frac{\hbar^2 k^2}{2m} - \gamma\hbar\omega,$$

and

$$\mathbf{k}' = \mathbf{k} - \gamma\mathbf{q}, \qquad \text{(C1)}$$

which lead to the following relationships between z, $\cos\theta$, and $\cos\theta_k$:

$$\cos\theta_k = \frac{\frac{1}{2}\left[(1+M) - \gamma M \frac{z}{K} - \frac{1}{4}\frac{z^2}{KS}\right]}{\left(1 - \gamma \frac{\cos\theta}{\sqrt{KS}} z + \frac{z^2}{4KS}\right)^{1/2}}, \quad \text{(C2)}$$

$$\begin{aligned}
\cos\theta &= \gamma \frac{\sqrt{KS}}{z}(1-M) + M\sqrt{\frac{S}{K}} \\
&\quad + \gamma \frac{z}{4\sqrt{KS}}, \qquad \text{(C3)}
\end{aligned}$$

where θ_k and θ are the angles between $\mathbf{k}$ and

$\mathbf{k}'$, and $\mathbf{k}$ and $\mathbf{q}$ (phonon wavevector), respectively. Substituting (C3) into (C2), we have

$$\cos\theta_k = \frac{\frac{1}{2}\left[(1+M)-\gamma M\frac{z}{K}-\frac{1}{4}\frac{z^2}{KS}\right]}{\sqrt{M}\left(1-\frac{\gamma z}{K}\right)^{1/2}}. \quad \text{(C4)}$$

Using this result, the delta function representing energy and momentum conservations, $\delta[\varepsilon(\mathbf{k}')-\varepsilon(\mathbf{k})]$, can be written as

$$\begin{aligned}&\delta[\varepsilon_j(\mathbf{k}')-\varepsilon_i(\mathbf{k})]\\ &=\delta[\varepsilon'_j-\varepsilon_i+\gamma\hbar\omega]\delta[\mathbf{k}'-\mathbf{k}+q]\\ &=\frac{\sqrt{S}}{\sqrt{K}}\frac{M}{k_BT}\frac{1}{z}\delta(\cos\theta_k-\cos\theta_0), \quad \text{(C5)}\end{aligned}$$

where $\cos\theta_0$ takes the value given in (C4).

The integration limits are determined by the condition that $|\cos\theta|<1$. For the phonon emission process, the lower and upper limits are given by

$$\begin{aligned}z_1&=2\sqrt{S}\left\{-G_\pm\pm[G_\pm^2+K(M-1)]^{1/2}\right\},\\ z_2&=2\sqrt{S}\left\{-G_-+[G_-^2+K(M-1)]^{1/2}\right\}, \quad \text{(C6)}\end{aligned}$$

respectively, where the upper and lower signs correspond to $M>1$ and $M\leq 1$, respectively, and $G_\pm = M\sqrt{S}\pm\sqrt{K}$. When $M\ll 1$, there is a thres hold in K that must be exceeded in order for emission to be possible. By demanding that the argument of the square root be positive and that z_1 and z_2 be positive, we have

$$K\geq S(1+\sqrt{1-M})^2. \quad \text{(C7)}$$

For transitions from the heavy to light hole band, this requires that $K\geq 3.66S$. For $M=1$ (intraband transition) and $M>1$, this condition reduces to $K\geq S$. For the absorption process the integration limits are given by

$$\begin{aligned}z_1&=2\sqrt{S}\left\{G_\mp\pm[G_\mp^2+K(M-1)]^{1/2}\right\},\\ z_2&=2\sqrt{S}\left\{G_++[G_+^2+K(M-1)]^{1/2}\right\}. \quad \text{(C8)}\end{aligned}$$

APPENDIX D

For warped band, r_H depends on the degree of warping as well as scattering mechanisms [7]

$$r_H = r_S\cdot r_A. \quad \text{(D1)}$$

Here r_S is the scattering factor, which is obtained by $r_S = <\tau^2>/<\tau>^2$, and r_A is the band anisotropy factor. We use the values $r_A=0.659$ for the heavy hole band and $r_A=0.996$ for the light hole band [7]. Once drift mobilities (μ_1 and μ_2) and Hall factors (r_{H1} and r_{H2}) for each band are calculated, the combined Hall mobility (μ_H) and Hall factor (r_H) for the two bands are determined, respectively, by

$$\mu_H = \frac{p_1\mu_1^2 r_{H1}+P_2\mu_2^2 r_{H2}}{p_1\mu_1+p_2\mu_2}, \quad \text{(D2)}$$

$$r_H = \frac{\mu_H}{\mu_d}. \quad \text{(D3)}$$

where p_1 and p_2 are hole densities in heavy and light hole bands, respectively, and μ_d is the combined drift mobility of holes.

REFERENCES

[1] B. R. Nag, *Electron Transport in Compound Semiconductors.* Berlin: Springer-Verlag, 1980.

[2] D. C. Look, *Electrical Characterization of GaAs Materials and Devices,* John Wiley & Sons, 1989.

[3] D. M. Szmyd, M. C. Hanna, and A. Majerfeld, "Heavily doped GaAs:Se. II. Electron mobility," *J. Appl. Phys*., vol. 68, no. 5, pp. 2376-2381, 1990.

[4] T. Brudevoll, T.A. Fjeldly, J. Baek, and M.S. Shur, "Scattering rates for holes near the valence-band

edge in semiconductors," *J. Appl. Phys.,* vol. 67, no. 12, pp. 7373-7382, 1990.

[5] M. Costato and L. Reggiani, "Scattering probabilities for holes," *Phys. Stat. Sol. (b)*, vol. 58, pp. 47-54, 1973.

[6] M. Costato, C. Jacoboni, and L. Reggiani, "Hole transport in polar semiconductors," *Phys. Stat. Sol. (b)*, vol. 52, pp. 461-473, 1972.

[7] J. D. Wiley, Mobility of holes in III-V compounds, in *Semiconductors and Semimetals,* Vol. 10, New York: Academic, 1975. pp. 1-89.

[8] M. Kohler, "Transporterscheinungen im elektronengas," *Z. Phys*., vol. 125, pp. 679-693, 1949.

[9] D. J. Howarth and E. H. Sondheimer, "The theory of electronic conduction in polar semiconductors," *Proc. Roy. Soc. London,* vol. A219, pp. 53-74, 1953.

[10] H. Ehrenreich, "Electron scattering in InSb," *J. Phys. Chem. Solids*, vol. 2, pp. 131-149, 1957; "Transport of electron in intrinsic InSb," *ibid.* vol. 9, pp. 129-148, 1959.

[11] D. L. Rode, "Electron mobility in direct-gap polar semiconductors," *Phys. Rev.,* vol. 2, no. 4, pp. 1012-1024, 1970.; D.L. Rode and S. Knight, "Electron transport in GaAs," *ibid.* vol. 3, no. 8, pp. 2534-2540, 1971.

[12] K. Takeda, N. Matsumoto, A. Taguchi, H. Taki, E. Ohta, M. Sakata, "Hole mobility of GaAs, GaP, and $GaAs_{1-x}P_x$ mixed-compound semiconductrors," *Phys. Rev. B*, vol. 32, no. 2, pp. 1101-1111, 1985.

[13] K. Brennan and K. Hess, "Theory of high-field transport of holes in GaAs and InP," *Phys. Rev. B*, vol. 29, no. 10, pp. 5581-5590, 1984.

[14] J. D. Wiley, "Polar mobility of holes in III-V compounds," *Phys. Rev. B*, vol. 4, no. 8, pp. 2485-2493, 1971.

[15] W. Walukiewicz, L. Pawlowicz, J. Lagowski, and H.C. Gatos, *Proc. of the Conference on Semi-Insulating III-V Materials*, Evian 1982 (edited by S.M.Ebeid and B.Tuck), Shiva Nantwich, U.K., 1982. pp. 121.

[16] W. Walukiewicz, "Carrier scattering by naive defects in heavily doped semiconductors," *Phys. Rev. B*, vol. 41, no. 14, pp. 10218-10220, 1990.

[17] D. Kranzer, "Polar mobility of electrons and holes," *Phys. Stat. Sol. (b)*, vol. 50, pp. K109-K113, 1972.

[18] D. Kranzer, "Hall and drift mobility of polar p-type semiconductors: I. Theory," *J. Phys. C: Solid State Phys.,* vol. 6, pp. 2967-2976, 1973.

[19] W. Bernard, H. Roth, and W. D. Straub, "Galvanomagnetic studies of degenerate gallium-doped germanium: nonparabolic energy bands with variable warping," *Phys. Rev.,* vol. 132, no. 1, pp. 33-46, 1963.

[20] J. R. Lowney and H. S. Bennett, "Majority and minority electron and hole mobilities in heavily doped GaAs," *J. Appl. Phys.,* vol. 69, no. 10, pp. 7102-7110, 1991.

[21] H. S. Bennett and J. R. Lowney, "Calculated majority- and minority-carrier mobilities in heavily doped silicon and comparisons with experiment," *J. Appl. Phys.,* vol. 71, no. 5, pp. 2285-2296, 1992.

[22] H. J. Lee and D. C. Look, "Hole transport in pure and doped GaAs," *J. Appl. Phys.,* vol. 54, no. 8, pp. 4446-4452, 1983.

[23] M. C. Hanna, Z. H. Lu, and A. Majerfeld, "Very high carbon incorporation in metalorganic vapor phase epitaxy of heavily doped p-type GaAs," *Appl. Phys. Lett.,* vol. 58, p. 164, 1991.

[24] C. R. Abernathy, S. J. Pearton, R. Caruso, F. Ren, and J. Kovalchik, "Ultrahigh doping of GaAs by carbon during metalorganic molecular beam epitaxy," *Appl. Phys. Lett.,* vol. 55, p. 1750, 1989.

[25] L. W. Yang, P. D. Wright, P. R. Brusenback, S. K. Ko, A. Kaleta, Z. H. Lu, and A. Majerfeld, *Electronics Lett.,* vol. 27, p. 1145, 1991.

[26] B. W. Kim and A. Majerfeld, "Electronic and intersubband optical properties for p-type

GaAs/AlGaAs superlattices for infrared photodetectors," *J. Appl. Phys.,* vol. 77, no. 9, pp. 4552-4563, 1995.

[27] A. Majerfeld, Z. H. Lu, B. W. Kim, E. Mao, S. A. Dickey, and E. G. Oh, to appear in the *Proc. of the First International Symposium on Long Wavelength Infrared Detectors*, *184th Electrochemical Society Meeting,* New Orleans, Louisiana, Oct. 1993.

[28] J. Appel, "Interband electron-electron scattering and transport phenomena in semiconductors," *Phys. Rev*., vol. 125, no. 6, pp. 1815-1823, 1962.

[29] H. Brooks and C. Herring, "Scattering by ionized impurities in semiconductors," *Phys. Rev*., vol. 83, p. 879, 1951.

[30] B. W. Kim and A. Majerfeld, "Analysis of ionized-impurity-scattering relaxation time and mobility by the phase-shift method for two interacting valence bands," *Phys. Rev. B*, vol. 51, no. 3, pp. 1553-1561, 1995.

[31] P. Lawaetz, "Symmetry principles in the theory of transport properties with special reference to p-type germanium," *Phys. Rev*., vol. 166, no. 3, pp. 763-769, 1968.

[32] F. Szmulowicz and F. L. Madarasz, "Angular dependence of hole-acoustic-phonon transition rates in silicon," *Phys. Rev. B*, vol. 26, no. 4, pp. 2101-2112, 1982.

[33] F. Szmulowicz and F. L. Madarasz, "Deformation-potential-theory calculation of the acoustic-phonon-limited conductivity and Hall mobilities for p-type silicon," *Phys. Rev. B*, vol. 27, no. 4, pp. 2605-2608, 1983.

[34] F. Szmulowicz and F. L. Madarasz, "Full-Boltzmann-equation solutions of the acoustic-phonon-limited conductivity and Hall mobilities for p-type silicon and germanium," *Phys. Rev. B*, vol. 27, no. 10, pp. 6279-6295, 1983.

[35] F. Szmulowicz, "Calculation for optical- and acoustic-phonon-limited conductivity and Hall mobilities for p-type silicon and germanium," *Phys. Rev. B*, vol. 28, no. 10, pp. 5943-5963, 1983.

[36] F. Szmulowicz, "Acoustic and optical-phonon-limited mobilities in p-type silicon within the deformation-potential theory," *Appl. Phys. Lett.,* vol. 43, no. 5, pp. 485-487, 1983.

[37] F. Szmulowicz, "Calculation of the mobility and the Hall factor for doped p-type silicon," *Phys. Rev. B*, vol. 34, no. 6, pp. 4031-4047, 1986.

[38] J. M. Hinckley and J. Singh, "Monte Carlo studies of ohmic hole mobility in silicon and germanium: Examination of the optical phonon deformation potential," *J. Appl. Phys*., vol. 76, no. 7, pp. 4192-4200, 1994.

[39] M. Dr, K. Unterrainer, and E. Gornik, "Effect of valence-band anisotropy and nonparabolicity on total scattering rates for holes in nonpolar semiconductors," *Phys. Rev. B*, vol. 49, no. 19, pp.13991-13994, 1994.

[40] J. S. Blakemore, *Key Papers in Physics Gallium Arsenide*, edited by J.S. Blakemore. New York: American Inst. of Phys., 1987.

[41] J. M. Ziman, *Principles of the Theory of Solids*, 2nd ed. Cambridge Univ. Press, 1972. pp. 231.

[42] E. O. Kane, "Energy band structure in p-type germanium and silicon," *J. Phys. Chem. Solids*, vol.1, pp. 82-99, 1956.

[43] S. A. Stokman, G. E. Hofler, J. N. Baillargeon, K. C. Hsieh, K. Y. Cheng, and G. E. Stillman, "Characterization of heavily carbon-doped GaAs grown by metalorganic chemical vapor deposition and metalorganic molecular beam epitaxy," *J. Appl. Phys*., vol. 72, no. 3, pp. 981-987, 1992.

B. W. Kim received the Ph. D. degree in electrical and computer engineering from University of Colorado, Boulder, Colorado in 1993. From 1983 to 1988, he was involved in the development of a digital switching system in ETRI. Since he joined the ETRI again in 1994, he has been working on III-V compound-semiconductor optical switches based on the strain-induced piezoelectric effects. His research interests include theoretical physics of compound semiconductor materials and optoelectronic devices.

A. Majerfeld is a professor in Department of Electrical and Computer Engineering of University of Colorado, Boulder, Colorado. His research interests include physics and technology of III-V semiconductor materials and optoelectronic devices, including MOVPE growth, MQW-IR photodetectors, PNPN lasers, optical waveguides, HBTs, electrical and optical characterization, and nanometric technology.